Bogdan SAPIŃSKI*, Jacek SNAMINA**

VIBRATION CONTROL CAPABILITIES OF A CANTILEVER BEAM WITH A MAGNETORHEOLOGICAL FLUID

SUMMARY

This paper presents an analysis of dynamic characteristics of a cantilever beam with a magnetorheological (MR) fluid. The beam consists of two aluminium outer layers and MR fluid layer placed between them. Due to MR fluid control capabilities both damping and stiffness of the beam can be changed simultaneously. The simple model of three-layered structure is assumed. Vibration characteristics of the beam are predicted for various magnetic field strength and a simple control algorithm based on switching of the beam stiffness is proposed. The results of calculations illustrate the vibration control capabilities of the MR adaptive beam at various level of magnetic strength.

Keywords: *magnetorheological fluid, cantilever beam, vibration control*

MOŻLIWOŚCI STEROWANIA DRGANIAMI BELKI WSPORNIKOWEJ Z CIECZĄ MAGNETOREOLOGICZNĄ

W pracy przedstawiono analizę własności dynamicznych belki z cieczą magnetoreologiczną (MR). Belka składa się z trzech warstw. Dwie zewnętrzne warstwy wykonano z aluminium, a przestrzeń pomiędzy nimi wypełniono cieczą MR. Sztywność i tłumienność belki można zmieniać dzięki zależnym od pola magnetycznego własnościom cieczy. Do obliczeń przyjęto prosty model belki trójwarstwowej. Wyznaczono podstawowe charakterystyki dynamiczne belki dla różnych wartości natężenia pola magnetycznego. Otrzymane wyniki potwierdzają możliwości sterowania drganiami belek zawierających warstwę cieczy MR.

Słowa kluczowe: *belka wspornikowa, ciecze magnetoreologiczne, sterowanie drganiami*

1. INTRODUCTION

Magnetorheological (MR) fluids are materials whose rheological properties can be rapidly varied under the action of magnetic fields. A lot of research has been focused on application of MR fluids in vibration damping.

In the paper we study vibration control capabilities of a three-layered cantilever beam with MR fluid. This beam can be considered as a structural element whose damping and stiffness characteristics are adjusted by a magnetic field. Research data of such beams are reported in the literature e.g. (Weiss *et al*. 1994, US Patent 1994, Dai and Yalcinitis 1998, Yalcinitis and Dai 1998, Sun *et al*. 2003).

We focus on transverse vibration of the beam assuming that the MR fluid is in the pre-yield regime and its property can be described by complex shear modulus. This modulus depends on magnetic field strength (Weiss *et al*. 1994, Nakano *et al*. 1997). In order to investigate vibration control capabilities of the beam we develop the finite element model (FEM model).

2. BASIC PROPERTIES OF MAGNETORHEOLOGICAL FLUIDS

MR fluids are non-colloidal suspensions consisting of high concentration magnetically polarizable particles suspended in a non-magnetic liquid carrier. The particles of MR fluids, made of iron or iron oxides, have a size of the order of a few microns in diameter, typically (3, 5) mm. The rheological properties of MR fluids depend on the concentration, particle size, shape distribution, properties of the carrier fluid, additional additives, applied strength and temperature.

MR fluids exhibit an ability to reversibly change from free-flowing, linear viscous liquids to semi-solids with a controllable yield strength when exposed to magnetic field. The change of MR fluid rheological behavior increases monotonically with a magnetic field strength and a response time is the order of milliseconds. The explanation of MR fluid behavior is shown in Figure 1.

The detailed analysis of rheological behavior reveals two regimes, known as pre-yield regime and post-yield regime (Jolly *et al.* 1999). Both regimes are associated with two characteristic shear stresses, i.e. dynamic shear yield stress and static shear yield stress which depend on magnetic field strength (Ginder and Davis 1995). In the pre-yield regime, the MR fluid behaves like a solid gel. The part of the energy transformed from the system to MR fluid is stored while another portion is dissipated in the form of heat. In the post--yield regime MR fluid displays visco-plastic properties. Typical MR fluids yield stresses are in the range (50, 100) kPa for applied magnetic fields strength in the range (150, 250) kA/m.

* Department of Process Controll, AGH University of Science and Technology, Krakow; deep@agh.edu.pl

** Institute of Applied Mechanics, Cracow University of Technology, Krakow; js@mech.pk.edu.pl
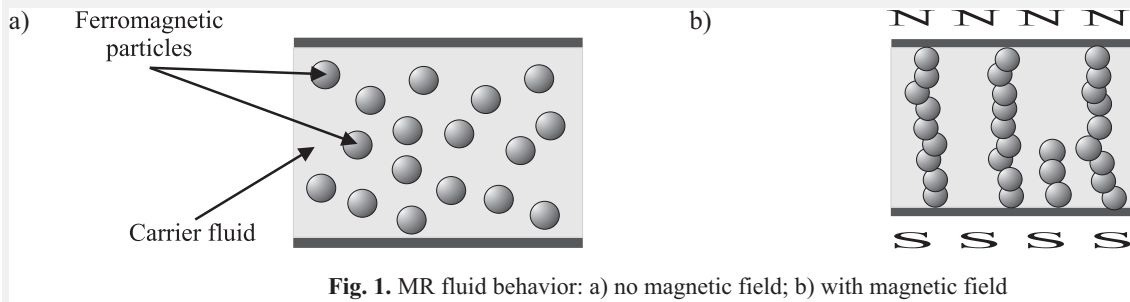
Fig. 1. MR fluid behavior: a) no magnetic field; b) with magnetic field

3. EQUATIONS OF THE BEAM

The beam to be considered consists of two aluminium outer layers and MR fluid layer placed between them. The configuration and schematic diagram of the beam is shown in Figure 2. The following designations are introduced: l is the length of the beam, b is the width of the beam, h and h_0 are outer layers and MR fluid layer thickness.
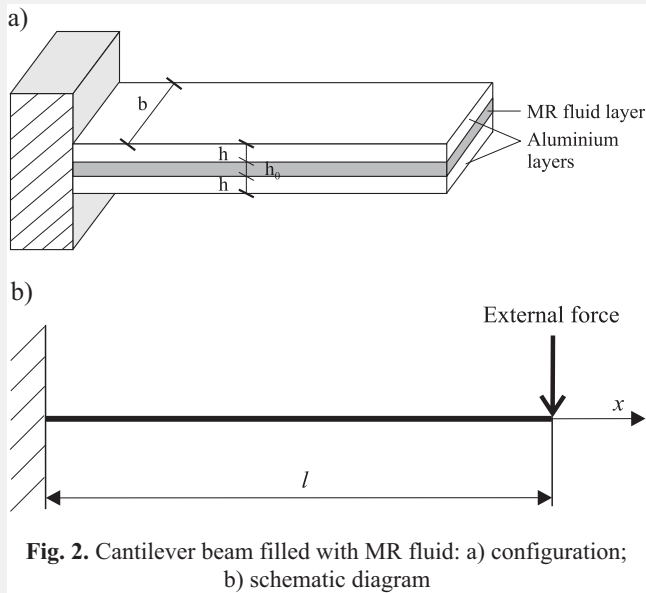

Fig. 2. Cantilever beam filled with MR fluid: a) configuration; b) schematic diagram

Fig. 3. Segment of the beam in deformed state: a) displacements; b) internal forces

The outer layers are assumed to be elastic and their stiffness is significantly higher than MR fluid layer. Energy dissipation in MR fluid is primarily due to shear deformation. Thus we assume only shear deformation in MR-fluid layer whereas shear deformation in the outer layers are negligible. No slip occurrs at the interface of the MR-fluid and outer layers. The inertia forces of transverse motion is dominant, rotary inertia of all layers is negligible. The various assumptions and various boundary conditions in three-layered structures are presented in the literature e.g. (Sun and Lu 1995).

The positions of small segments of each layer before deformation and after deformation of the beam are presented in Figure 3.

Taking into account all assumptions we can express strains of each layer. The shear strain of MR-fluid layer is given by:

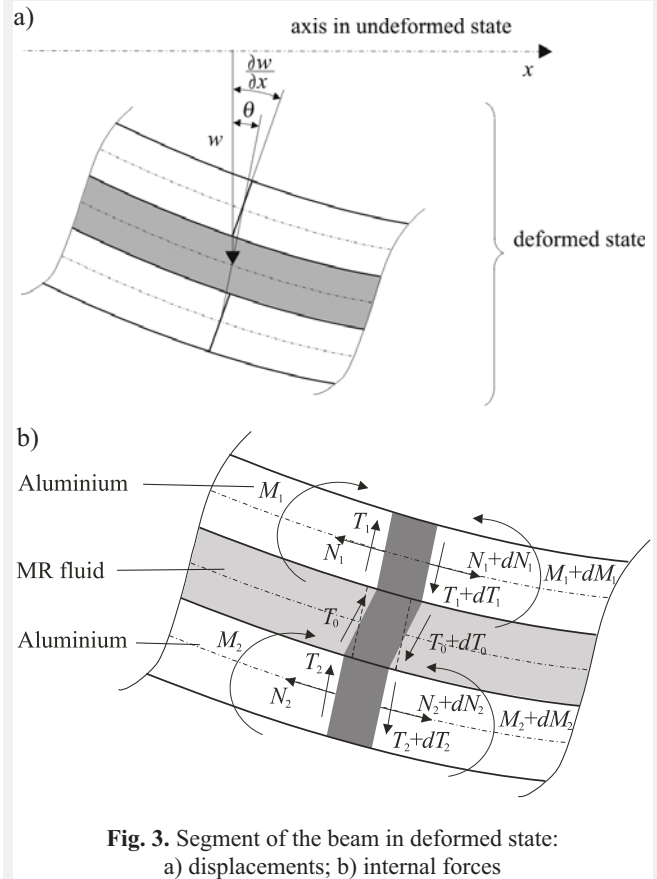$$\gamma = \left(\frac{h}{h_0} + 1 \right)\left(\frac{\partial w}{\partial x} - \theta(x,t) \right) \qquad (1)$$

In order to describe the phenomena in MR fluid layer during vibration of the beam the complex stress and strain have been introduced. The complex cycling stress τ and strain γ in MR fluid layer (in pre-yield regime) can be related using the complex shear modulus G^*:

$$\tau = G^* \gamma \qquad (2)$$

The modulus G^* represents simultaneously the stiffness and damping property of MR fluid layer. This modulus can only be employed if the solution takes the complex exponential forms as in the case of harmonic motion. Assuming, that the strain is described by real value, the complex shear stress has the real part proportional to shear strain and the imaginary part that implies the existence of a resistive stress which has the amplitude proportional to the strain and it is in counterphase with the strain velocity.

The real part of complex shear modulus is called storage modulus and the imaginary part is called loss modulus. The maximal value of potential energy stored per unit volume in one strain cycle is proportional to storage modulus and the corresponding energy dissipated is proportional to loss modulus. The ratio of loss modulus to storage modulus is called the loss factor.

In further consideration we use the following relationships for the storage modulus G_s and the loss modulus G_l *vs.* magnetic field strength value H after (Sun *et al*. 2003):

$$G_s = (5 \times 10^{-11} \times H^2 + 4.5 \times 10^{-6} \times H + 5.78 \times 10^{-1}) \times 10^6 \tag{3}$$

$$G_l = (5.5 \times 10^{-13} \times H^2 + 4.8 \times 10^{-8} \times H + 6.31 \times 10^{-3}) \times 10^6$$

The graphical interpretation of Eqs (3) in the range necessary for our calculations is shown in Figure 4.

The kinetic energy is a sum of kinetic energies of outer layers and MR fluid layer. The potential energy is a sum of strain energy of outer layers and the potential energy associated with storage modulus of MR fluid layer.

Taking into account the assumed deformations of each layer, the kinetic energy can be expressed as

$$T = \frac{1}{2} \int_{V_1} (\dot{u}_1^2 + \dot{w}_1^2) \rho \, dV + \frac{1}{2} \int_{V_0} (\dot{u}_0^2 + \dot{w}_0^2) \rho_0 \, dV + $$
$$+ \frac{1}{2} \int_{V_2} (\dot{u}_2^2 + \dot{w}_2^2) \rho \, dV \tag{4}$$

where $\dot{u}_i$ and $\dot{w}_i$ are longitudinal and transversal components of velocity, V_i are volumes of layers, indices $i = 0, 1, 2$ relate to MR fluid layer and two (upper and bottom) aluminium layers respectively, ρ is density of aluminium, ρ_0 is density of MR fluid.

The outer layers are bent and stretched. Bending is a result of overall beam deformation and stretching is a result of interaction of MR fluid layer. Thus the extension strain ε is only one non-zero component of strain. The strain energy accumulated in two outer layers can be written as:

$$V_s = \frac{1}{2} \int_{V_1} E \varepsilon_1^2 \, dV + \frac{1}{2} \int_{V_2} E \varepsilon_2^2 \, dV \tag{5}$$

where E is Young modulus of aluminium.

The complex potential energy of MR fluid layer using complex shear modulus G^* can be expressed as:

$$V_{MR} = \frac{1}{2} \int_{V_1} G^* \gamma^2 \, dV \tag{6}$$

According to previous consideration Eq. (6) represents the energy stored in MR fluid layer (real part) and the energy dissipated in MR fluid layer (imaginary part).

The differential equation of the beam cycling motion can be derived using Hamilton's principle. The resulting equations are difficult to solve analytically and for this reason we introduce FEM model of the beam.

4. FINITE ELEMENT MODEL

In order to create the FEM model of the beam we apply 2-D line element. It has two nodes with translational (in transversal direction) and rotational degrees of freedom.

The displacement inside the element is interpolated using the corresponding nodal values by:

$$\begin{bmatrix} w_e \\ \theta_e \end{bmatrix} = \begin{bmatrix} N_w^T & 0 \\ 0 & N_\theta^T \end{bmatrix} \begin{bmatrix} q_w \\ q_\theta \end{bmatrix} \tag{7}$$

where: $q_w = [w_1 \, \varphi_1 \, w_2 \, \varphi_2]^T$, $q_\theta [\theta_1 \, \theta_2]^T$ are nodal displacement vectors (displacements and rotations at the origin of element is signed by subscripts 1, displacements and rotations at the end point of element by subscripts 2), N_w, N_θ are the vectors of shape functions. We assumed that the shape functions used to create N_w are known as Hermite cubics and the shape functions used to create N_θ are linear functions.

In order to derive the mass matrix of the element M_e, the kinetic energy of the element should be expressed as a quadratic form of the nodal velocities

$$T = [\dot{w}_e^T \, \dot{\theta}_e^T] M_e \begin{bmatrix} \dot{w}_e \\ \dot{\theta}_e \end{bmatrix} \tag{8}$$

Since the modulus representing properties of MR fluid layer is complex, the stiffness matrix of element K_e^* is complex too.
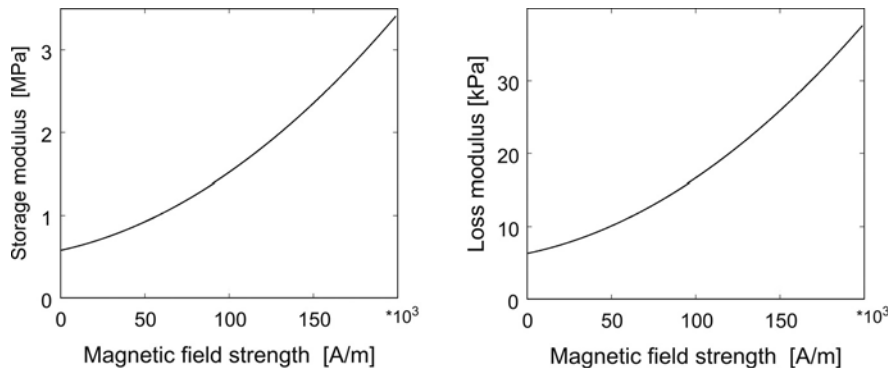

Fig. 4. Storage modulus and loss modulus *vs.* magnetic field strength

The real part of K_e^* can be derived taking into account the strain energy of outer layers and the storage component of complex energy of MR fluid layer:

$$V_s + \mathrm{Re}(V_{MR}) = \frac{1}{2}[w_e^T \ \theta_e^T]\,\mathrm{Re}(K_e^*)\begin{bmatrix} w_e \\ \theta_e \end{bmatrix} \qquad (9)$$

The energy dissipated in MR fluid layer can be expressed using imaginary part of stiffness matrix K_e^* as follows:

$$\mathrm{Im}(V_{MR}) = \frac{1}{2}[w_e^T \ \theta_e^T]\,\mathrm{Im}(K_e^*)\begin{bmatrix} w_e \\ \theta_e \end{bmatrix} \qquad (10)$$

The motion of the overall system is defined in terms of nodal displacements and rotations. They were arranged in generalized displacements vector $u = [u_1, u_2, ..., u_N]^T$. Equations of beam vibration can be finally written in a matrix form as

$$M\ddot{u} + K^* u = Q \qquad (11)$$

where the mass matrix M and stiffness matrix K^* for the overall beam are obtained from element mass matrices and element stiffness matrices in the assembling process. The vector of nodal forces Q for the complete system is obtained by calculating the virtual work of the force applied to the beam.

5. RESULTS OF NUMERICAL CALCULATIONS

The main purpose of calculations was to estimate the influence of magnetic field strength on free and forced vibrations. The results of calculations should characterize vibration control capabilities of MR fluid layer in a beam structure.

The calculations were performed for the following beam parameters: length $l = 0.4$ m, width $b = 0.025$ m, thickness of outer layers and MR fluid layer $h = h_0 = 0.001$ m, density of aluminium (outer layers) 2.7×10^3 kg/m^3, density of the MR fluid 3.5×10^3 kg/m^3, Young modulus of aluminium 0.7×10^{11} Pa.

At first we calculated the natural frequencies and corresponding dimensionless modal damping coefficient. Next the time history of displacement of the end point of the beam was determined. The results are shown in Figure 5 and in Tables 1, 2 and 3.
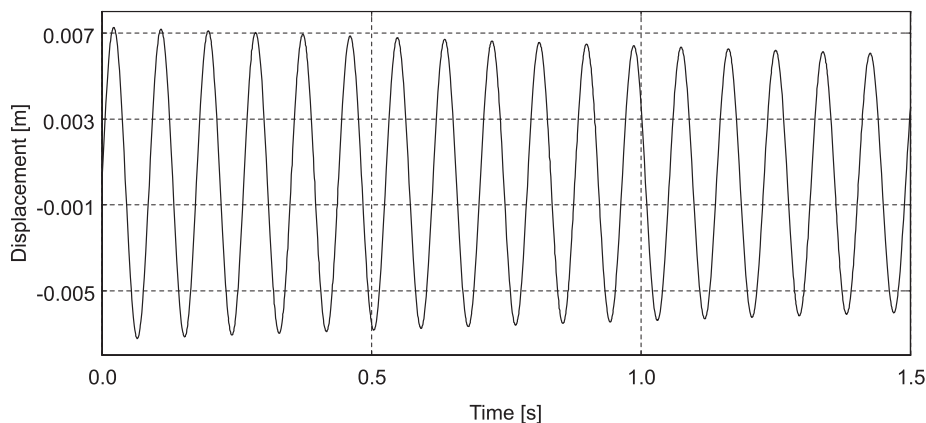
Table 1
Natural frequencies

Mode number	Natural frequency [Hz]
1	4.00
2	25.10
3	70.39
4	138.58
5	231.04
6	345.69

The natural frequencies listed in Table 1 were calculated for the beam with the dummy fluid that has not magneto-rheological properties but same density as MR fluid. In this case the energy of beam is conserved and therefore modal damping coefficients are equal to zero.

Table 2 shows the results obtained when the magnetic field strength is equal to 8×10^4 A/m. Table 3 presents the results of calculations when the magnetic field strength is equal to 16×10^4 A/m.

Table 2
Natural frequencies and modal damping coefficients

| Mode number	Natural frequency [Hz]	Modal damping coefficient [–]
1	11.40	1.80×10^{-3}
2	46.20	2.57×10^{-3}
3	102.37	2.43×10^{-3}
4	173.83	1.86×10^{-3}
5	266.52	1.39×10^{-3}
6	381.02	1.03×10^{-3}

Fig. 5. Displacement of the beam end point

Table 3
Natural frequencies and modal damping coefficients

Mode number	Natural frequency [Hz]	Modal damping coefficient [–]
1	12.58	1.23×10^{-3}
2	54.73	2.61×10^{-3}
3	121.46	2.80×10^{-3}
4	200.45	2.52×10^{-3}
5	298.11	2.08×10^{-3}
6	415.69	1.69×10^{-3}

The calculations reveal that when the magnetic field strength increases, natural frequency and the modal damping coefficient increase too. This regularity is associated with relation between magnetic field strength and complex shear modulus (Eq. 3). The MR fluid becomes more rigid and its viscosity is larger as magnetic field strength increases. The values of modal damping coefficient are small even for strong magnetic fields therefore the efficiency of vibration suppression is rather small.

Figure 5 shows displacement time history of the beam end point damped by MR fluid layer in the presence of magnetic field of 8×10^4 A/m. We assumed the motion with the first natural mode.

Next we calculated the forced vibration. We assumed that the beam was excited by the concentrated force applied at the end of the beam. The displacement was calculated at point where the force was applied for various excitation frequencies. In Figure 6 we show frequency response curves for magnetic field strength of: 8×10^4 A/m (solid line), 16×10^4 A/m (dash line).
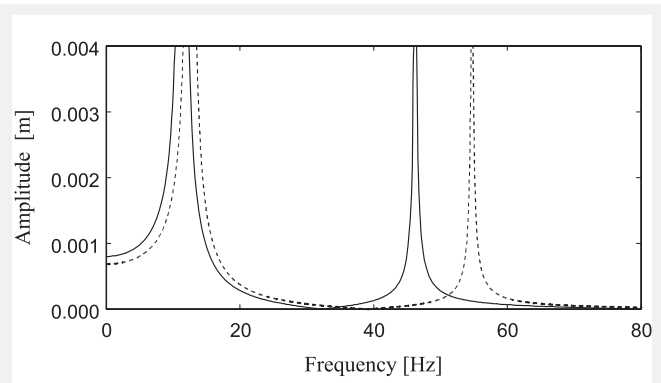
Fig. 6. Frequency response curves of the beam end point for various magnetic field strength

6. BEAM MOTION UNDER MAGNETIC FIELD SWITCHING

In order to reduce vibrations in more effective way, the concept of switched stiffness can be applied (Walsh and Lamancusa 1992, Ramaratman and Nader 2006). This concept can be adopted in the considered beam, however, it requires the control subsystem to be used. Figure 7 shows the relation between the motion of the beam end point and stiffness switching. The stiffness of beam is changed by switching the magnetic field strength. Analyzing the displacement and velocity it is easy to explain the dissipation of energy. When the displacement increases the stiffness is high. At the moment when the displacement reaches its maximum, the stiffness is switched to low value. Since the displacement does not change, the part of potential energy is lost. Thus the total energy of beam is reduced. Then the displacement decreases. At the moment when displacement is equal to zero, the stiffness is switched to high value. By this switching the total energy is
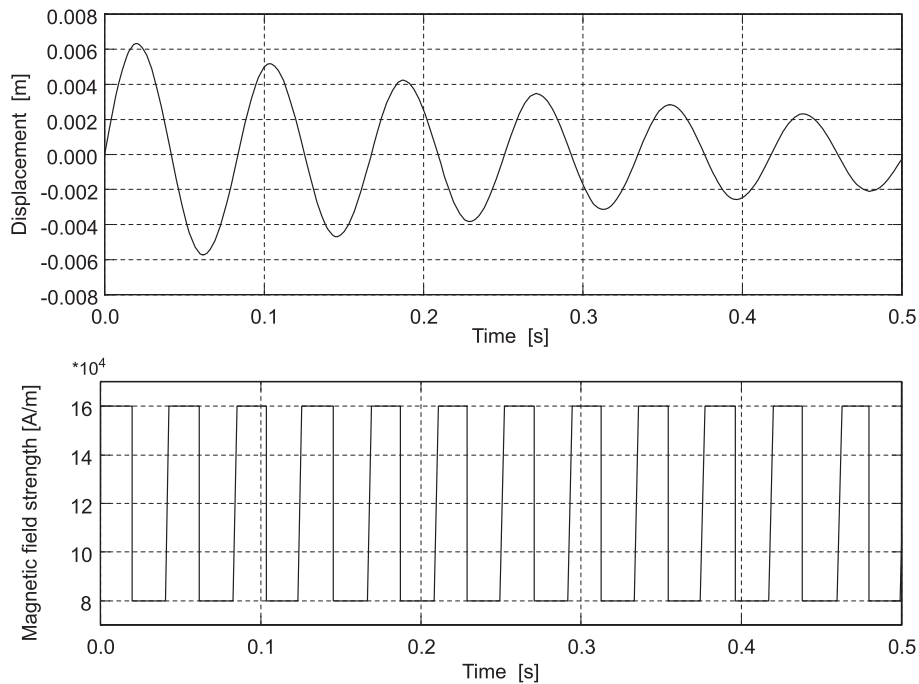
Fig. 7. Displacement of the beam end point under magnetic field switching

conserved because the potential energy in this position is equal to zero (the total energy of the beam is equal to the kinetic energy). Then the process of switching is repeated. In general high stiffness value is taken when the system is moving away from its equilibrium position while low stiffness value is taken when the system is returning to its equilibrium position.

Taking into account the displacement and velocity for free vibration with any mode the control law can be written as:

$$w \cdot \dot{w} \geq 0 \Rightarrow K_s = (K_s)_{high}$$
$$w \cdot \dot{w} < 0 \Rightarrow K_s = (K_s)_{low} \tag{12}$$

If the product of displacement and velocity is positive, the stiffness must be high. In the opposite case the stiffness must be low.

In Figure 7 we show displacement of the beam end point executing free vibration with the first mode and corresponding magnetic field strength switching (switched between 8×10^4 A/m and 16×10^4 A/m).

7. SUMMARY

The study explores vibration control capabilities of a three--layered cantilever beam with MR fluid. In order to describe the phenomena in MR fluid layer during transverse vibration of the beam we introduced the complex shear modulus and developed FEM model.

Numerical study revealed vibration control capabilities of the beam. MR fluid layer enables to change both stiffness and damping of the beam under the action of magnetic field. The modal damping coefficients increase when the magnetic field strength increases. Furthermore, the natural frequencies shift to higher frequencies. However, even for high value of magnetic field strength the modal damping coefficients are not satisfactory enough. The main reason of small damping is the location of MR layer close to the axis of the beam. Strains in MR layer are small and therefore the dissipation of energy is insufficient. In order to significantly increase the damping of the beam, an appropriate switching strategy of magnetic field strength should be employed. The equivalent modal damping coefficient in the controlled system is several times greater than modal damping in the uncontrolled system.

The next step of our research is to develop a more accurate model of the beam filled with MR fluid which allows us to predict its real behavior. This model will be verified experimentally.

REFERENCES

Dai H., Yalcinitas M. 1998: *Vibration Suppression Capabilities of Magnetorheological Materials in Adaptive Structures*.

Ginder J.M., Davis L.C. 1995: *Shear stress in magnetorheological fluids: models and measurement*s. Proceedings of 5th International Conference: ER, MR Suspensions Associated Technology, Sheffield, United Kingdom.

Jolly M.R., Bender W., Carlson J.D. 1999: *Properties and Applications of Commercial Magnetorheological Fluids*. Journal of Intelligent Material Systems and Structures, vol. 10.

Nakano M., Yamamoto H., Jolly M.R. 1997: *Dynamic Viscoelasticity of a Magnetorheological Fluid in an Oscillatory Slit Flow*. Proceedings of 6th International Conference on ERF and MRS and Their Applications, Yonezawa, Japan.

Ramaratman A., Nader J. 2006: *A switched stiffness approach for structural vibration control: theory and real-time implementation*. Journal of Sound and Vibration, 291, pp. 258–274.

Sun Q., Zhou J.X., Zhang L. 2003: *An adaptive beam model and dynamic characteristics of magnetorheological materials*. Journal of Sound and Vibration, 261, pp. 465–482.

Sun C.T., Lu Y.P. 1995: *Vibration Damping of Structural Elements*. Prentice-Hall PTR.

United States Patent No. 5,547,049, 1994: *Magnetorheological Fluid Composite Structures*.

Walsh P.L., Lamancusa J.S. 1992: *A variable stiffness vibration absorber for minimization of transient vibration*. Journal of Sound and Vibration, 120 (4), pp. 1291–1305.

Weiss K.D., Carlson J.D., Nixon D.A. 1994: *Viscoelestic properities of magneto- and electrorheological fluids*. Journal Intelligent Material Systems and Structures, pp. 772–782.

Yalcinitis M., Dai H. 1998: *Performance comparison of magnetorheological and electrorheological materials in adaptive structural applications*. Adaptive Structure and Materials Systems ASME, vol. 83, 49–61.